

Co(II) and Fe(III) Complexes of a Hydrazone Derived from 4-Aminoantipyrine and Pentan-2,4-Dione: Synthesis, Characterization and Antimicrobial Studies

Ndidiamaka Justina Agbo, Pius Onyeoziri Ukoha, *Uchechukwu Susan Oruma

Coordination Chemistry and Inorganic Pharmaceuticals Unit

Department of Pure and Industrial Chemistry

University of Nigeria, Nsukka, Enugu State, Nigeria

*Corresponding Author: susan.oruma@unn.edu.ng

Accepted: July 23, 2024. Published Online: August 2, 2024**ABSTRACT**

Co(II) and Fe(III) complexes of 3-E-[2-(1,5-dimethyl-3-oxo-2-phenyl-2,3-dihydro-1*h*-pyrazol-4-yl)hydrazinylidene]pentane-2,4-dione (HDPP) were synthesized. The synthesized compounds were characterized by UV-Vis, IR, NMR spectroscopic methods, elemental analysis and conductivity measurements. Antibacterial activity of the compounds against *P. aeruginosa*, *S. aureus*, *E. coli*(Eco 6), *E. coli*(13), *B. subtilis*, *S. pneumoniae*, *P. mirabilis*, *S. intermedius*, and *K. pneumoniae* were assessed *in vitro*. HDPP crystallized in orthorhombic crystal system, space group pbca, with 8 molecules per unit cell, and unit cell parameters $a = 28.501(4) \text{ \AA}$, $\alpha = 90^\circ$, $b = 15.0494(19) \text{ \AA}$, $\beta = 90^\circ$. Spectral studies indicate that HDPP is tridentate and coordinates to Fe(III) ions via C=O of acetylacetone, N-H and C=O of pyrazolone ring; whereas for Co(II) ions, C=O of acetylacetone and C=O of pyrazolone ring were involved in coordination. The Fe(III) complex was cationic, whereas the ligand and Co(II) complexes were neutral according to the conductivity values of HDPP and complexes. HDPP showed no activity against test organisms, but the complexes showed various degrees of sensitivities against the test organisms at $10 \mu\text{g}/\text{cm}^3$. Acute toxicity (LD₅₀) tests showed that HDPP was non-toxic.

Key words: Hydrazone, spectroscopy; X-ray crystallography; Co(II) and Fe(III) complexes; Antibacterial activity.

INTRODUCTION

A class of chemical compounds known as hydrazones has the structure $\text{R}^1\text{R}^2\text{C}=\text{N}-\text{NH}_2$. Because they have the functional group $=\text{N}-\text{NH}_2$ in place of the oxygen $=\text{O}$, they are related to ketones and aldehydes [1]. Due to the presence of alpha-active hydrogen atoms in hydrazones, they have

been found to be more reactive than carbonyl groups [2]. They have been synthesized by previous researchers [2-7]. Hydrazones have proved to be versatile candidates in complex formation [4, 8- 9], pharmacology [2, 3, 10-11] and agrochemicals[12-13]. Various biological effects are demonstrated by them, including anticonvulsant, antidepressant, analgesic, anti-inflammatory, antiplatelet, antimalarial, antimicrobial, antimycobacterial, antitumoral, vasodilator, antiviral, and schistosomiasis properties [2, 14].

Microorganisms are the causative agents of sicknesses in man. The scourge due to various sicknesses is still prevalent because of the emergence of resistant strains of pathogenic microbes to already existing drugs, hence the need for newer and effective drugs. Complexes of Co(II) and Fe(III) with different ligands have been shown to exhibit antimicrobial activities [15-18]. However, very scanty reports exist as regards Co(II) and Fe(III) complexes of hydrazones of β -diketones [5-7]. In view of the noted pharmaceutical applications of hydrazones, Co(II) and Fe(III) complexes of a novel β -diketones hydrazone namely 3-E-[2-(1,5-dimethyl-3-oxo-2-phenyl-2,3-dihydro-1H-pyrazol-4-yl)hydrazinylidene]pentane-2,4-dione, HDPP were synthesized and characterized. Their acute toxicity and *in vitro* antibacterial activity were also studied.

MATERIALS AND METHODS

Chemicals purchased from Zayo-Sigmas were pentan-2,4-dione, 4-aminoantipyrine, iron(III) chloride-hexahydrate and cobalt(II) chloride. They were used without additional purification. UV-Visible data were obtained on Cecil UV-Visible spectrophotometer (CE2041, Europe). The chemicals were analyzed using KBr discs on a Perkin-Elmer FTIR spectrometer(1600 series, USA) for FTIR data, Bruker AVIII-400 NMR spectrometer for NMR data, and Heraeus Carlo Erba 1108-CHN analyzer for micro analytical data. X-ray crystallography data of HDPP was run on goniometer(Supernova, CCD, Poland) of Kappa geometry and CCD diffractometer (Xcalibur, X-ray source: ENHANCE and/or ULTRA, Poland) equipped with Mo, $K\alpha$ source. After accounting for polarization and absorption effects, HDPP was examined to determine the space group. Clinical isolates from humans included *P. aeruginosa*, *B. subtilis*, *S. aureus*, *E. coli* (*Eco.6*), *E. coli* (*Eco.13*), *S. pneumoniae*, and *S. intermedius*; clinical isolates from pigs

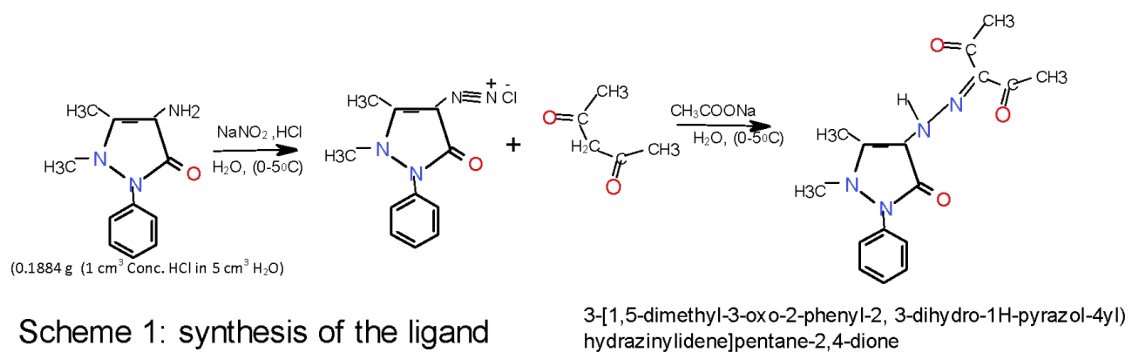
included *P. mirabilis* and *K. pneumoniae*. The University of Nigeria Nsukka's Department of Biochemistry provided the albino mice and rats.

Synthesis of the ligand, 3-E-[2-(1,5-dimethyl-3-oxo-2-phenyl-2,3-dihydro-1h-pyrazol-4-yl)hydrazinylidene]pentane-2,4-dione

The method reported by Heinosuke [19] was adopted for synthesis of the ligand. 4-Aminoantipyrene (0.1884 g; 9.86×10^{-4} mol) was dissolved in dilute HCl and diazotized with NaNO_2 at $< 5^\circ\text{C}$ under stirring. The diazonium salt was poured into a mixture of 6.0×10^{-4} mol dm^{-3} solution of pentan-2,4-dione and 2.5g; 3.04×10^{-2} mol/ 150 cm^3 of CH_3COONa under constant stirring. After the product precipitated, it was washed using methanol/water solvent (1:1). It was recrystallized with methanol and dried over CaCl_2 in a desiccator (Scheme 1).

Synthesis of the complexes

The metal complexes were prepared by the reported method [20]. Metal salts were mixed separately with HDPP in 2:1 mole ratio in ethanol. The mixtures were refluxed for 6 h at 60°C . The precipitates formed were filtered, washed, then dried over CaCl_2 in a desiccator.



Antibacterial screening of HDPP and the complexes

Using the Agar-well diffusion method, the compounds in DMSO were first subjected to a preliminary antibacterial screening [21-22]. The test microorganisms were injected into 0.1 cm^3 broth cultures on both Sabouraud Dextrose Agar (SDA) and Nutrient Agar plates that had already been prepared. Wells (5 mm in diameter and 2.5 mm deep) were drilled into the infected plate using a sterile cork borer. For the purpose of evaluating the compounds' antibacterial properties, a 50 mg sample of each was dissolved in DMSO and diluted evenly to produce

concentrations between 0.156 and 10 $\mu\text{g}/\text{cm}^3$. Standard antibiotics: Ciprofloxacin, Ampicilin and Gentamycin served as positive control, whereas the negative control was sterile DMSO. After incubation at 37 °C, the inhibition zone diameters (IZD) were determined. The antilog of the intercept on the y-axis of IZD^2 versus Log (concentration) plot gave the minimum inhibitory concentration (MIC).

Acute Toxicity (LD₅₀) studies

The ethical conduct of research involving animals has been validated to have been met in all mouse-based investigations (Approval Reference Number: FVM-UNN-IACUC-2023-11/132). With the aid of the Lorke method [23], the LD₅₀ was determined. After 24h of acclimatization, 144 mice of both sexes were utilized. The mice were placed in three groups of five each and given between 10 to 1000 mg/kg body weight of test compounds separately via 3% v/v normal saline. After 24 h observation, death pattern was noted and used for the second phase where between 1900 and 5000 mg/kg body weights of compounds were offered. Pattern of lethality after 24 h was recorded.

RESULTS AND DISCUSSION

Single Crystal XRD Data of HDPP

The single crystal data and structure refinement of HDPP is shown in Table 1 whereas selected bond length and hydrogen bonds are presented in Table 2. The ORTEP diagram and Crystal packing are presented in Figures 1.0 and 2.0 respectively. The results showed HDPP to have orthorhombic crystals of Pbc_a space group and unit cell dimension $a = 28.501(4) \text{ \AA}$, $\alpha = 90^\circ$, $b = 15.0494(19) \text{ \AA}$, $\beta = 90^\circ$, and $c = 7.3234(9) \text{ \AA}$, $\gamma = 90^\circ$ for $z=8$.

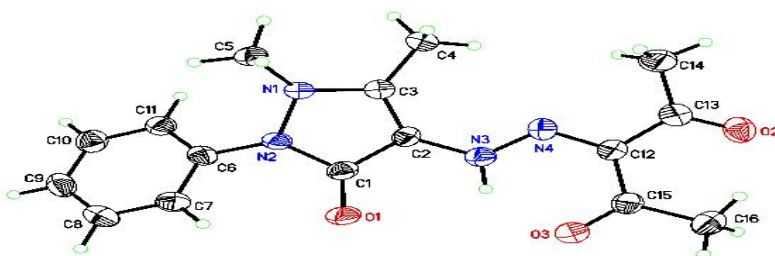


Fig. 1.0: The ORTEP diagram of HDPP

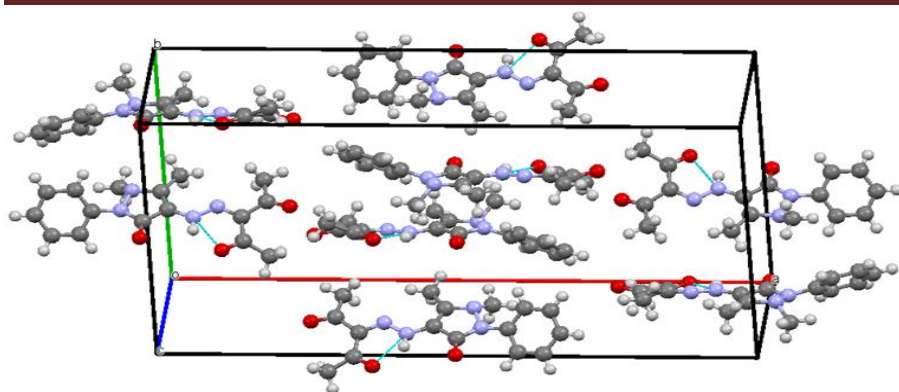


Fig. 2.0: Crystal packing of the HDPP

Table 1: Crystal data and structure refinement details of HDPP

Identification code	HDPP
Empirical formula	C ₁₆ H ₁₈ N ₄ O ₃
Formula weight	314.34
Temperature	100(2) K
Wavelength	0.71073 Å
Crystal system	Orthorhombic
Space group	Pbca
Unit cell dimensions	$a = 28.501(4)$ Å, $\alpha = 90^\circ$ $b = 15.0494(19)$ Å, $\beta = 90^\circ$ $c = 7.3234(9)$ Å, $\gamma = 90^\circ$
Volume	3141.2(7) Å ³
Z	8
Density (calculated)	1.329 g.cm ⁻³
Absorption coefficient (μ)	0.095 mm ⁻¹
F(000)	1328
Crystal color, habit	yellow, blocks
θ range for data collection	2.859 to 27.655°
Index ranges	$-35 \leq h \leq 35$, $-19 \leq k \leq 19$, $-8 \leq l \leq 9$
Reflections collected	24321
Independent reflections	3563 [$R_{int} = 0.1288$]
Completeness to $\theta = 25.242^\circ$	99.3 %
Refinement method	Full-matrix least-squares on F^2
Data / restraints / parameters	3563 / 0 / 213
Goodness-of-fit on F^2	1.039
Final R indices [$ I > 2\sigma(I) $]	$R_1 = 0.0604$, $wR_2 = 0.1450$
R indices (all data)	$R_1 = 0.1032$, $wR_2 = 0.1683$
Extinction coefficient	n/a
Largest diff. peak and hole	0.235 and -0.297 e ⁻ .Å ⁻³

Table 2: Selected Bond lengths [\AA] and Bond angles [$^\circ$].

atom-atom	distance	atom-atom-atom	Angle
O(1)-C(1)	1.235(3)	C(3)-N(1)-N(2)	106.64(15)
O(3)-C(15)	1.236(3)	N(2)-N(1)-C(5)	114.55(16)
N(1)-N(2)	1.415(2)	C(1)-N(2)-C(6)	125.03(17)
N(2)-C(1)	1.385(3)	N(4)-N(3)-C(2)	122.38(19)
N(3)-N(4)	1.310(2)	C(2)-N(3)-H(3N)	118.8
N(3)-H(3N)	0.8800	O(1)-C(1)-N(2)	126.0(2)
C(1)-C(2)	1.433(3)	N(2)-C(1)-C(2)	104.79(17)
C(3)-C(4)	1.482(3)	C(3)-C(2)-C(1)	109.65(18)
O(2)-C(13)	1.228(3)	C(2)-C(3)-N(1)	108.84(18)
N(1)-C(3)	1.382(3)	N(1)-C(3)-C(4)	120.81(18)
N(1)-C(5)	1.473(3)	C(3)-C(4)-H(4B)	109.5
N(2)-C(6)	1.419(3)	C(3)-C(4)-H(4C)	109.5
N(3)-C(2)	1.393(3)	H(4B)-C(4)-H(4C)	109.5
N(4)-C(12)	1.321(3)	C(3)-N(1)-C(5)	119.00(16)
C(2)-C(3)	1.358(3)	C(1)-N(2)-N(1)	109.51(16)
C(4)-H(4A)	0.9800	N(1)-N(2)-C(6)	121.06(16)
C(4)-H(4C)	0.9800	N(4)-N(3)-H(3N)	118.8
C(5)-H(5B)	0.9800	N(3)-N(4)-C(12)	119.87(19)
C(7)-C(8)	1.383(3)	O(1)-C(1)-C(2)	129.2(2)
C(8)-C(9)	1.375(3)	C(3)-C(2)-N(3)	133.2(2)
C(9)-C(10)	1.381(3)	N(3)-C(2)-C(1)	117.17(19)

Symmetry transformations used to generate equivalent atoms

The X-ray diffraction analysis of HDPP shows that HDPP crystallizes in orthorhombic space group $Pbca$ with $Z = 8$. The diffractogram recorded 24321 reflections for θ ranging between 2.859 to 27.650° with maxima at $\theta = 25.242^\circ$. From Table 2, and on the basis of bond lengths, C(1)-O(1), C(13)-O(2) and C(15)-O(3) are double bonds. The slightly higher value of C(15)-O(3) is due to the hydrogen bonding of O(3) to H(3) of N(3). Also N(3) - H(3)...O(3) hydrogen bonding is supported by N(3)- H(3) bond length of 0.8800 \AA . The single bond character of N(3) -N(4) bond length of $1.310(2) \text{ \AA}$ is a further proof of the formation of hydrazone with H-N-N-moiety instead of an azo compound with -N=N- group [24].

Physicochemical properties of the compounds.

The yield, melting point, color, texture and conductivity of the synthesized compounds are listed in Table 3.

Table 3: Physicochemical properties of HDPP and its complexes

Compound	% Yield	Colour	Texture	M. Pt(°C)	Molar. Cond.(Scm ⁻¹)
HDPP	56.22	Orange yellow	Powdery	138-140	3.8 x 10 ⁻⁷
[Co(HDPP) ₂ Cl ₂]	48.48	Black	Crystalline	123-124	32.54 x 10 ⁻⁶
[Fe(HDPP) ₂]Cl ₃	86.42	Brown	Crystalline	129-130	1.24 x 10 ⁻³
KCl	-	-	-	-	1.76 x 10 ⁻³
CuSO ₄	-	-	-	--	7.60 x 10 ⁻⁴

HDPP and its complexes were synthesized in moderate to high yields. The complexes were crystalline while HDPP is powdery. Conductivities of the complexes when compared to HDPP and controls, CuSO₄ (2:2 electrolyte) and KCl (1:1) electrolyte revealed that the values for cobalt(II) complex as well as HDPP were lower by between 70 to 10,000 units when compared to the controls. This is an indication that they are non-electrolytes. [Fe(HDPP)₂]Cl₃ has conductivity value close to that of KCl implying its electrolytic nature.

Elemental and mass spectral data

The elemental analysis data of these compounds show that the amount of carbon, hydrogen and nitrogen are close to the experimentally determined values. HDPP (C: % Calc 61.15, % experimental values 61.55; H: % Calc 5.73, % experimental values 5.44; N: % Calc 17.83, % experimental values 17.77); [Co(HDPP)₂Cl₂] (C: % Calc 56.06, % experimental values 56.10; H: % Calc 4.75, % experimental values 4.79; N: % Calc 14.78, % experimental values 15.83); [Fe(HDPP)₂]Cl₃ (C: % Calc 53.53, % experimental values 52.84; H: % Calc 4.55, % experimental values 4.19; N: % Calc 14.17, % experimental values 14.98). It also affirms the formulae given to the synthesized compounds as HDPP, [Co(HDPP)₂Cl₂] and [Fe(HDPP)₂]Cl₃ respectively. HDPP has molecular formula of C₁₆H₁₈N₄O₃ and molecular mass of 314.345g/mol. This is in agreement with the molecular ion peak (Fig. 1) of 339.580 which represents (M+Na)⁺. The absence of (M-N₂)⁺ peak in the spectrum of HDPP proves that HDPP is a hydrazone and not azo compound [24].

Electronic spectral data of the compounds

The HDPP and its complexes' electronic spectra were captured in DMSO. These are presented in Figs. 2-4 in supplementary materials. HDPP showed a maximum absorption at 413.00 nm with molar absorptivity of $265.975 \text{ dm}^3\text{mol}^{-1}\text{cm}^{-1}$. This absorption is attributed to $n-\pi^*$ intra ligand transition. In $[\text{Fe}(\text{HDPP})_2]\text{Cl}_3$, one absorption band was observed at 406.000 nm with molar absorptivity of $430.54 \text{ dm}^3\text{mol}^{-1}\text{cm}^{-1}$, whereas $[\text{Co}(\text{HDPP})_2\text{Cl}_2]$ absorbed at 411 and 455 nm with molar absorptivities of $627.33 \text{ dm}^3\text{mol}^{-1}\text{cm}^{-1}$ and $610.08 \text{ dm}^3\text{mol}^{-1}\text{cm}^{-1}$ respectively. These bands were assigned to d – d transitions of the metals respectively. The shift in absorption bands in the complexes is due to complexation which disrupts the electronic structure of the ligand [25].

Infrared spectral data of the compounds

The vibrational frequencies of HDPP and its complexes are shown in Figs. 5-7 in supplementary materials. The broad bands (cm^{-1}) at 3437 in HDPP shifted to 3429 for $[\text{Fe}(\text{HDPP})_2]\text{Cl}_3$, 3419 for $[\text{Co}(\text{HDPP})_2\text{Cl}_2]$, and were assigned to $\nu(\text{N-H})$ stretch [26]. The shifts indicate the involvement of the N-H group in ligation to the metal ions without deprotonation [20]. The carbonyl stretching frequency ($\nu(\text{C=O})$ stretch of acetylacetone) appeared at 1820 cm^{-1} in HDPP but shifted to 1756 cm^{-1} in $[\text{Fe}(\text{HDPP})_2]\text{Cl}_3$ and 1768 cm^{-1} in $[\text{Co}(\text{HDPP})_2\text{Cl}_2]$. The shifts to lower frequencies indicates involvement of the C=O group in bonding to the metal. The pyrazolone ring $\nu(\text{C=O})$ frequency at 1668 cm^{-1} in HDPP shifted in all the complexes thereby implicating involvement of the pyrazolone C=O in ligation. The $\nu(\text{C=N})$ at 1593 cm^{-1} in HDPP remained unchanged in the complexes of Co(II) but shifted in Fe(III) complex. This suggests that in the Co(II) complex, the C=N and the H-N-N were not involved in bonding. The strong bands around $1188-1024 \text{ cm}^{-1}$ in HDPP and the complexes indicates $\nu(\text{N-N})$ stretching modes [6]. The lack of $\nu(\text{C-O})$ of enol in the spectrum suggests hydrazone structure for HDPP [6]. The appearance of new bands between $468-531 \text{ cm}^{-1}$ indicates the formation of metal to ligand bonds of the type M-O and M-N [20].

Nuclear Magnetic Resonance spectra of HDPP and its complexes

The ^1H and ^{13}C NMR spectra of HDPP and the complexes in CDCl_3 solution are shown in Figure 8-13 in supplementary materials. The signal at 1.8483 ppm (2H, S) shows trace H_2O impurity in the ligand. The proton chemical shift at 2.3704 ppm and 2.52265 ppm (3H,s) are

indicative of C-CH₃, N-CH₃ methyl protons of pyrazolone moiety [6]. The other methyl protons have chemical shifts at 3.1409 and 3.4564 ppm for the acetyl groups of the β-diketone. The chemical shift centered between 7.389-7.5359 ppm are due to aromatic protons.

¹³C-NMR spectrum of HDPP (Figure 9 supplementary materials) gave signals for 16 carbons. Signals at 129.85, 127.74 and 124.91 ppm represent carbon from two equivalent phenyl rings. Carbon at ortho-position, two at meta-position and one at para-position. The two methyl carbons on the pyrazolone ring have their signals at 11.89 (CH₃-C) and 22.44 ppm (CH₃-N). The two equivalent methyl carbons on the β-diketone moiety gave signal at 36.00 ppm whereas the two equivalent acetyl carbons had shift at 196.04 ppm. The signal at 173.10 ppm is due to the carbonyl group on the pyrazolone ring. The two other carbons of the pyrazolone ring gave signal at 144.57 and 134.66 ppm. Similar assignments had been suggested for such compound in earlier works [27, 28]. Due to paramagnetic affects, the ¹³C-NMR spectra of the complexes (Fig 11 and 13 in supplementary materials) suffered various degrees of distortions and shifts indicating formation of the complexes.

Structures of the compounds

Based on all the analytical data provided, it can be deduced that HDPP is a hydrazone with C-NH-N-C group and azo compound. HDPP is orthorhombic in its crystalline form and in its crystalline form hydrogen bonding occurs. HDPP is tridentate and coordinates to the metal ions through one acetyl oxygen, one hydrazinyl nitrogen and through the keto oxygen of the pyrazolone ring. The complexes formed are paramagnetic based on various degrees of distortion of their NMR spectra. Cobalt(II) complex is octahedral, non-ionic and has the formula [Co(HDPP)₂Cl₂]; complex formation did not lead to deprotonation of HDPP. Iron(III) complex is octahedral, cationic and has the formula [Fe(HDPP)₂]Cl₃; complex formation did not lead to deprotonation of HDPP.

On the basis of the accumulated analytical data, the following structures (Fig. 3 – 5) have been proposed for the compounds.

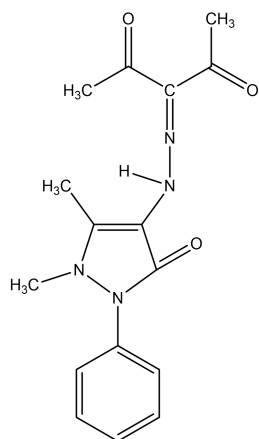


Fig. 3: Structure of HDPP

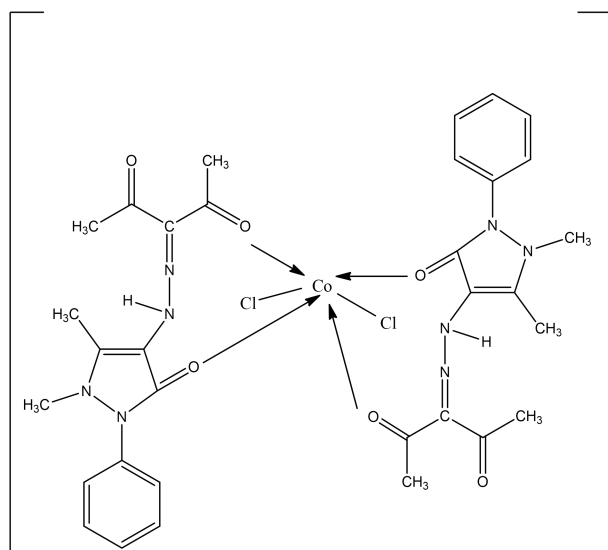


Fig. 4: Structure of $[Co(HDPP)_2Cl_2]$

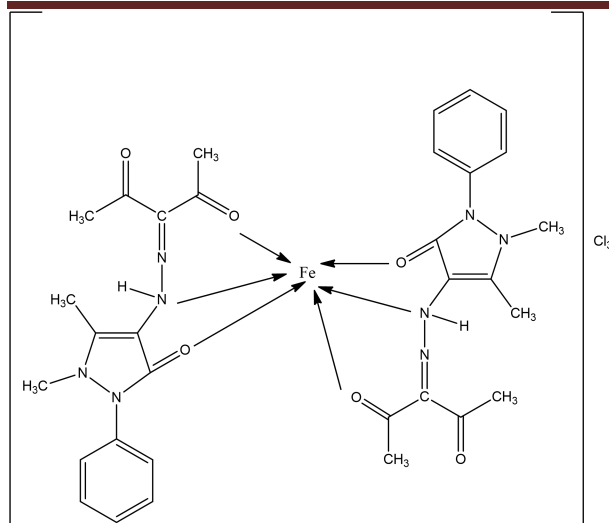


Fig.5: Structure of $[\text{Fe}(\text{HDPP})_2]\text{Cl}_3$

Antibacterial activities

Table 4 shows the zone of inhibition (mm) underlining the sensitivities of the microorganism to the test compounds as well as the controls. HDPP showed no activity against the bacteria strains. However, the complexes showed varying degrees of activities against the test organism. Of note is $[\text{Co}(\text{HDPP})_2\text{Cl}_2]$ with marked activity against all the bacteria except *P. aeruginosa* and *K. pneumoniae*. *P. aeruginosa* was not sensitive to any of the compounds. The varying degrees of activities could likely be due to the presence of the metal ions which modified the structure of HDPP thereby creating different motifs for binding to bacteria cells [29].

Table 4: Zone of Inhibitions of HDPP and its complexes

Compound	<i>B. subtilis</i>	<i>S. Pneumoniae</i>	<i>P. aeruginosa</i>	<i>E. coli (Eco6)</i>	<i>E. coli (Eco13)</i>	<i>S. aureus</i>	<i>P. mirabilis</i>	<i>S. Intermedius (G101)</i>	<i>K. pneumoniae</i>
HDPP	Nil	Nil	Nil	Nil	Nil	Nil	Nil	Nil	Nil
$[\text{Co}(\text{HDPP})_2\text{Cl}_2]$	24	25	Nil	20	23	21	24	29	Nil
$[\text{Fe}(\text{HDPP})_2]\text{Cl}_3$	18	Nil	Nil	Nil	Nil	16	Nil	19	Nil
Ampicilin	0.625	100	100	100	100	2.5	100	2.5	100
Gentamicin	0.1562	2.5	100	100	100	2.5	100	2.5	100
Ciprofloxacin	0.1562	2.5	50	6.25	50	2.5	100	2.5	100

Acute toxicity studies

Acute toxicity studies show that for mice administered with $[\text{Co}(\text{HDPP})_2\text{Cl}_2]$ and $[\text{Fe}(\text{HDPP})_2]\text{Cl}_3$ at 1000mg/kg led to some fatalities. Calculated LD_{50} for these compounds were <50 mg/kg inferring their high toxicity.

ACKNOWLEDGEMENT

The authors are grateful to the Department of Pure and Industrial Chemistry, University of Nigeria Nsukka for providing bench space and technical assistance.

CONCLUSION

A novel compound, HDPP, was synthesized and characterized via single crystal XRD, UV-Vis, IR, NMR spectroscopic methods, elemental analysis and conductivity measurements. Additionally, the Co(II) and Fe(III) complexes of it were synthesized and characterized. According to spectral analyses results, HDPP is tridentate and uses its ONO atoms to coordinate with the Co(II) and Fe(III) ions. This work is significant because, it has shown that the antibacterial activity of HDPP was enhanced on complexing with Co(II) ion. Also Co(II) complex of HDPP could serve as an antimicrobial drug after further tests. Modification of the structure of HDPP is proposed so as to reduce its toxicity level.

REFERENCES

1. Jerry, P. (1985). *Advanced Organic Chemistry. Reactions, Mechanisms and Structure*, 3rd edition, New York, Wiley. ISBN 9780471854722, OCLC 642506595.
2. Youssef, H. M., Khaleel, L. I., Azzam, M.A.& AbuEl-Reash, G. M. (2023). Mn(II) and Fe(III) complexes of N^1, N^2 -bis((E)-2-hydroxybenzylidene) oxalohydrazide: Synthesis, characterization, DFT studies, biological activity, and ion-flotation separation of Fe(III). *J. Mol. Struct.* 1287(5),135652.
3. Mohammed, M. A., Fetoh, A., Ali, T. A., Youssef, M. M., Abou El-Reash, Y. G. & Abu El-Reash, G. M. (2024). Co(II), Mn(II), and Fe(III) complexes of water-soluble hydrazone bearing 2-nicotinoylhydrazineylidene moiety: Preparation, characterization, cyclic voltammetry, computational and biological studies. *Appl. Organomet. Chem.* ???<https://doi.org/10.1002/aoc.7376>

4. Al-Shaalan, N. H. (2011). Synthesis, Characterization and Biological Activities of Cu(II), Co(II), Mn(II), Fe(II), and UO₂(VI) Complexes with a New Schiff Base Hydrazone: O-Hydroxyacetophenone-7-chloro-4-quinoline Hydrazone . *Molecules*. 16(10), 8629-8645. DOI: <https://doi.org/10.3390/molecules16108629>
5. Ravindran, R. (2004). Synthesis and characterisation of iron(III) complexes of 1,2-dihydro-1-phenyl-2,3-dimethyl-4-[2 ϕ ,4 ϕ -pentanedione-3 ϕ hydrazono]pyrazol-5-one, *Indian J. Chem.* 43A, 1245-1248.
6. Mohahan, K., Athira, C. J., Sindhu, Y. & Sujamol, M. S. (2009). Synthesis, spectroscopic characterization and thermal studies of some lanthanide(III) nitrate complexes with a hydrazone derivative of 4-aminoantipyrine. *J. rare earths*. 27(5), 705- 710.
7. Sarwar, N., Gao, P., Kondapally Seshasai, S. R., Gobin, R., Kaptoge, S., Di Angelantonio, E., Ingelsson, E., Lawlor, D. A., Selvin, E., Stampfer, M., Stehouwer, C. D. A., Lewington, S.; Pennells, L, Thompson, A., Sattar, N., White, I. R., Ray, K. K. & Danesh, J. (2010). Diabetes mellitus, fasting blood glucose concentration, and risk of vascular disease: a collaborative meta-analysis of 102 prospective studies. *Lancet*. 375(9733), 2215-22.
8. Manimaran, P., & Balasubramaniyan, S. (2019). Synthesis, Characterization and Biological Evaluation of Fe(III) and Cu(II) Complexes With 2,4-Dinitrophenyl Hydrazine and Thiocyanate ions. *Asian J. Chem.* 31(4), 780 – 784.
9. Issa, R. M., Abdel-Latif, S. A. & Abdel-Salam, H. A. (2001). *Synth. React. Inorg. Met.-Org. Chem.* 31, 95-105. DOI: 10.1081/SIM-100001935.
10. Sari, N., Nartop, D., Karci, F. & Disli, A. (2008). Novel Hydrazone Derivatives and Their Tetracoordinated Metal Complexes. *Asian J. Chem.* 20(3), 1975-1985.
11. Nawar, N., & Hosny, N. M. (2000). Synthesis, spectral and antimicrobial activity studies of o-aminoacetophenone o-hydroxybenzoylhydrazone complexes. *Trans. Met. Chem.* 25, 1- 8.
12. Ozmen, U. O. & Olgun, G. (2008). Synthesis, Characterization and antibacterial activity of new sulfonyl derivatives and their Ni(II) Complexes. *Spectrochim. Acta Part A*. 70, 641–645.
13. Ghaib, A., Ménager, S., , Vérité, P. & Lafont, O. (2007). Synthesis of variously 9,9-dialkylated octahydropyrimido [3,4-a]-s-triazines with potential antifungal activity. *IL Farmaco*. 57(89), 109 – 116.

14. Rollas, S. & Küçükgülzel, Ş. G. (2007). Biological activities of Hydrazone derivatives. *Molecules*. 12, 1910-1939.
15. Shukla, S. N., Gaur, P., Raidas, M. L. & Chaurasia, B. (2020). Tailored synthesis of unsymmetrical tetradentate ONNO schiff base complexes of Fe (III), Co (II) and Ni (II): Spectroscopic characterization, DFT optimization, oxygen-binding study, antibacterial and anticorrosion activity. *J. Mol. Struct.* 1202, 127362.
16. Salih, B. D., Dalaf, A. H., Alheety, M. A., Rashed, W. M. & Abdullah, I. Q. (2021). Biological activity and laser efficacy of new Co (II), Ni (II), Cu (II), Mn (II) and Zn (II) complexes with phthalic anhydride. *Mat. today: proceedings*. 43(2),869-874.
17. Abdel Aziz, A. A., Elantabli, F. M., Moustafa, H. & El-Medani, S. M. (2017). Spectroscopic, DNA binding ability, biological activity, DFT calculations and non linear optical properties (NLO) of novel Co(II), Cu(II), Zn(II), Cd(II) and Hg(II) complexes with ONS Schiff base. *J. Mol. Struct.* 1141(5), 563-576.
18. Kavitha, P., Chary, M. R., Singavarapu, B. V. V. A. & Reddy, K. L. (2016). Synthesis, characterization, biological activity and DNA cleavage studies of tridentate Schiff bases and their Co(II) complexes. *J. Saudi Chem. Soc.* 20(1), 69-80.
19. Heinosuke, Y. (1967). Infrared Analysis of 2-pyrazolin-5-one Derivatives, *Appl. Spect.* 23(1), 22-28.
20. El.Saied, F. A., Ayad, M. I., Issa, R. M. & Aly, S. A. (2001). Synthesis and charactersation of Iron(III), Cobalt (II), Nickel(II) and copper(II) Complexes of 4-formylazoaniline Antipyrine. *Polish. J. Chem.* 75(6), 773 – 783.
21. Mounyr, B., Moulay, S. & Saad, K. I. (2016). Methods for in vitro evaluating antimicrobial activity: A review. *J. Pharm. Anal.* 6(2), 71-79.
22. Heatley, N. G. (1944). A method for the assay of penicillin. *Biochem. J.* 38 (1), 61–65. DOI: 10.1042/bj0380061.
23. Lorke, D. (1983). A new approach to practical acute toxicity testing. *Arch. Toxic.* 54, 275-287.
24. Madhavan, S. N.; Dasan, A.; Raphael, S. J. (2012). “Synthesis, characterization, antifungal, antibacterial and DNA cleavage studies of some heterocyclic Schiff base metal complexes”. *J. Saudi Chem. Soc.* 16(1, 83-88.

25. Holm, R. H. (1961). Spectral and Magnetic Studies of Substituted Nickel(II) Salicylaldimine Complexes, in *Advances in the Chemistry of Coordination Compounds*; Kirschner, S., Ed.; MacMillan: New York, Pp. 341-349.
26. Hassan, F., Fayed, M. & Abdalla, S. J. (2020). Synthesis, Characterization, Antibacterial, and Antifungal Activities of Cobalt(II), Nickel(II) and Copper(II) Complexes with 3-thioacetyl-2-amino-1,4-naphthoquinone and 2-benzoyl-3-amino-1,4-naphthoquinone Ligands. *Open J. Inorg. Non-met. Mat.* 10: 45-61. DOI: 10.4236/ojinm.2020.104004.
27. Abdel-Wahab, B. F., Awad, G. E. & Badria, F. A. (2011). "Synthesis, antimicrobial, antioxidant, anti-hemolytic and cytotoxic evaluation of new imidazole-based heterocycles". *Eur. J. Med. Chem.* 46:1505 – 1511.
28. Ajayeoba, T. A., Akinyele, O. F. & Oluwole, A. O. (2017). Synthesis, Characterisation and Antimicrobial Studies of mixed Nickel(II) and Copper(II) complexes of Arylhydrazones with 2,2'-bipyridine and 1,10-phenanthroline. *Ife J. Sci.* 19(1), 119-132.
29. Maheshwari, D. G. & Shaikh, N. K. (2016). An overview on toxicity testing method. *Int. J. Pharm. Technol.* 8(2), 3834-3849.

SUPPLEMENTARY MATERIALS

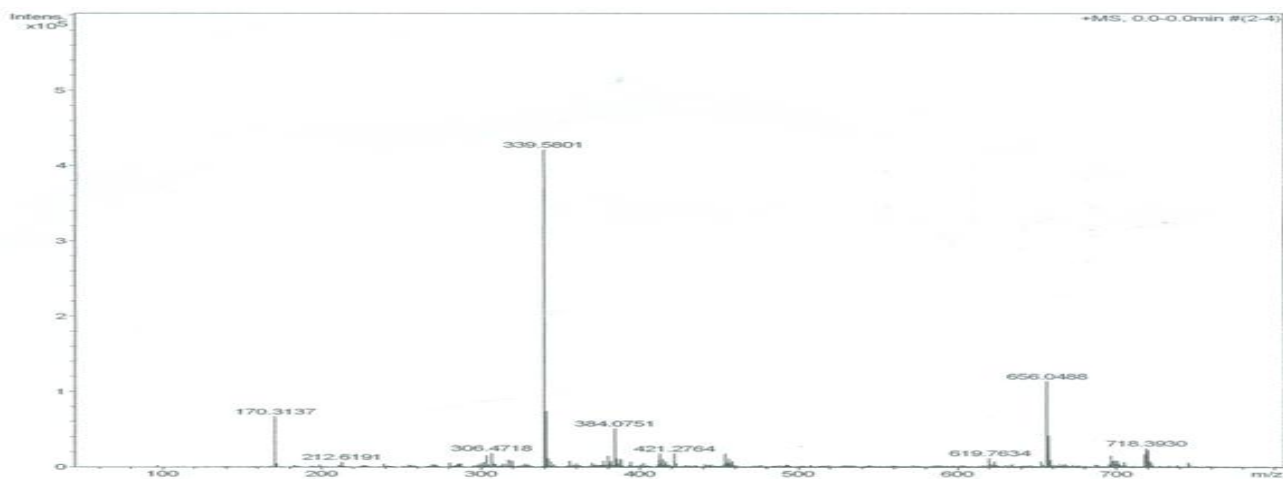


Fig 1: The mass spectrum of HDPP.

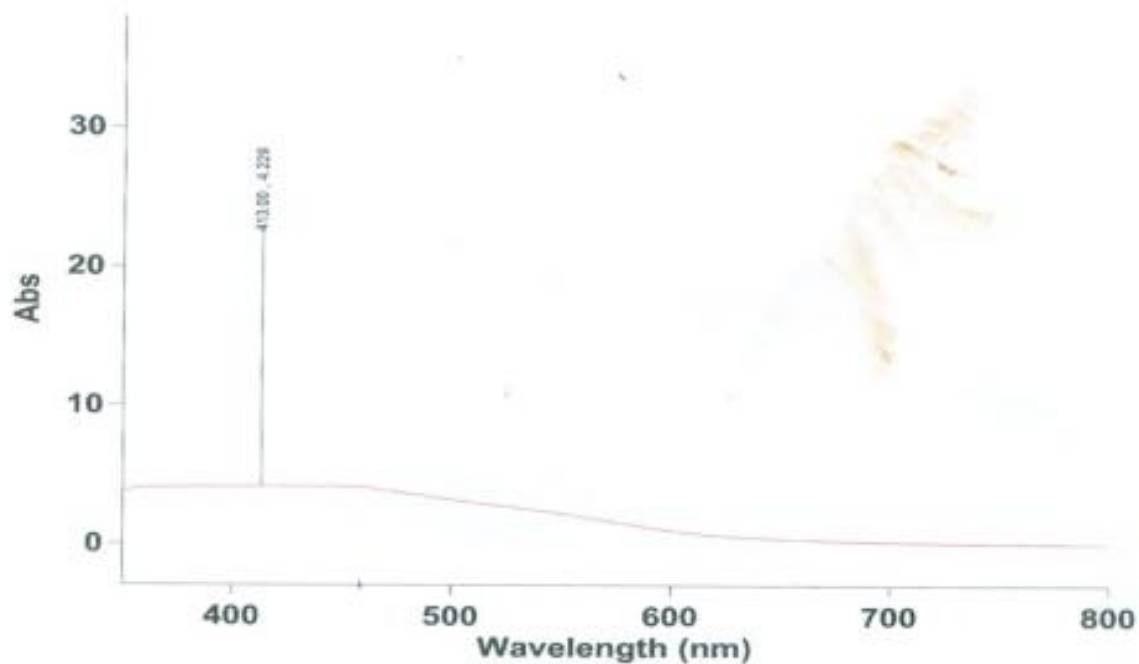


Fig. 2 : Electronic Absorption spectrum data of HDPP

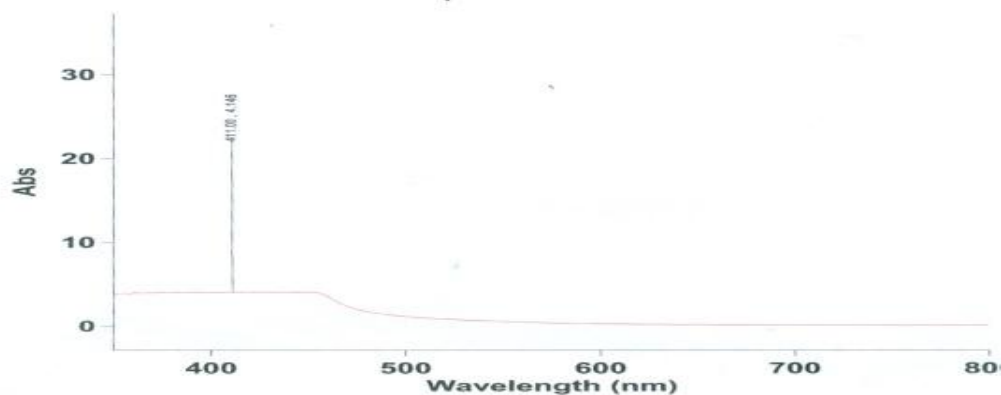


Fig. 3: Electronic spectrum data of [Co(DPP)₂]

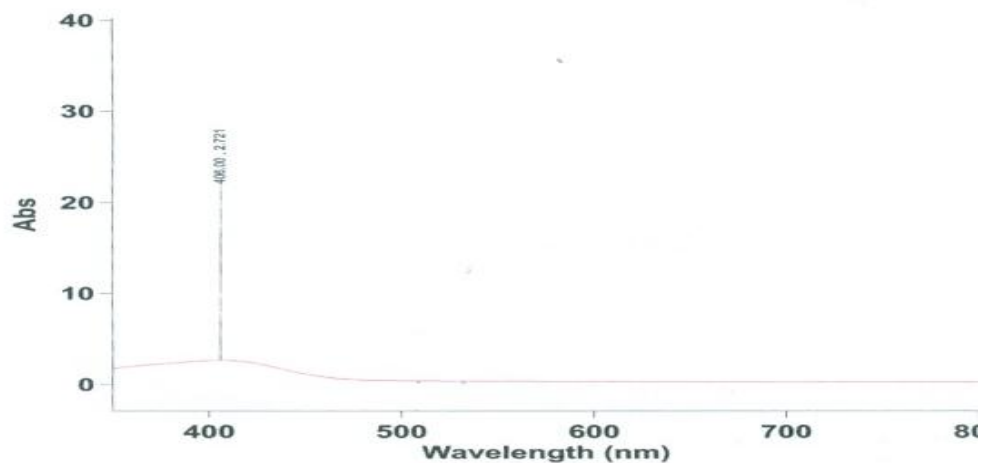


Fig. 4: Electronic spectrum data of [Fe(HDPP)₂]Cl

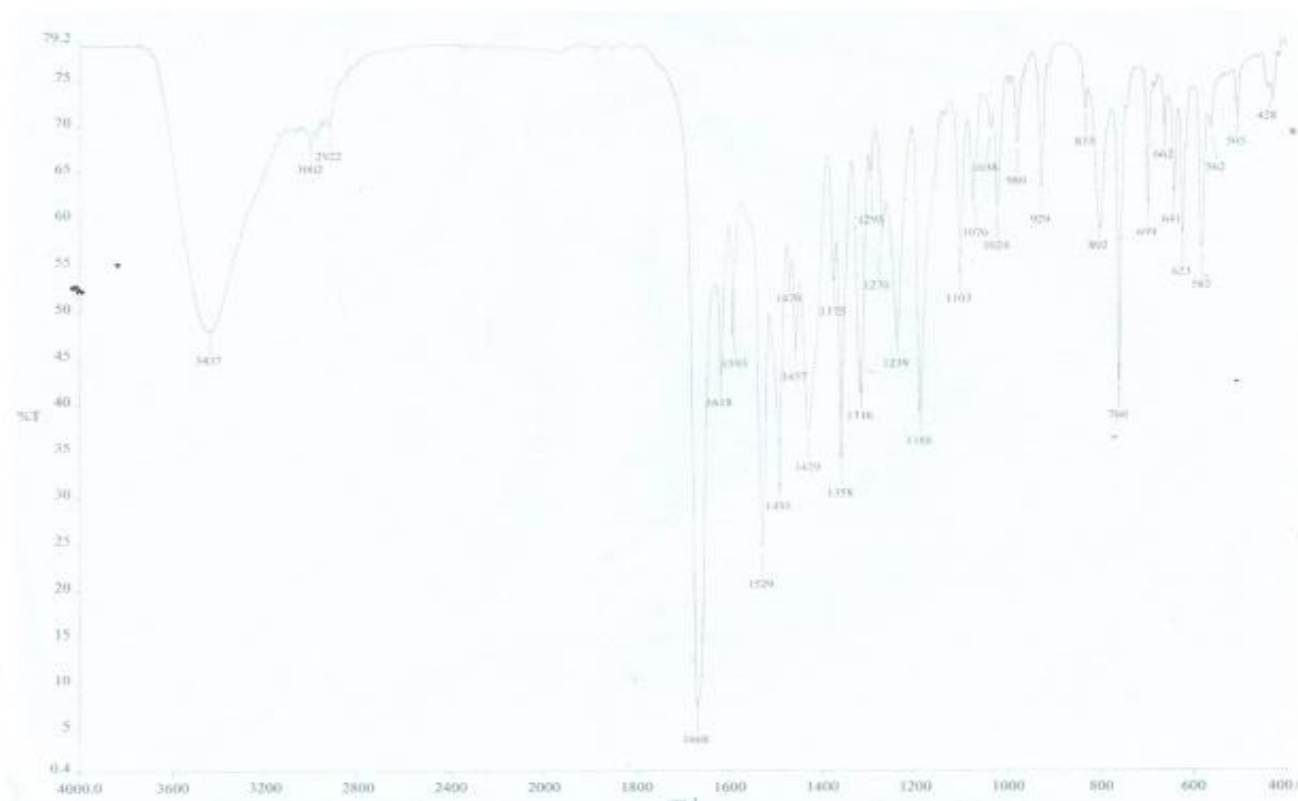


Fig. 5: IR Spectrum of HDPP

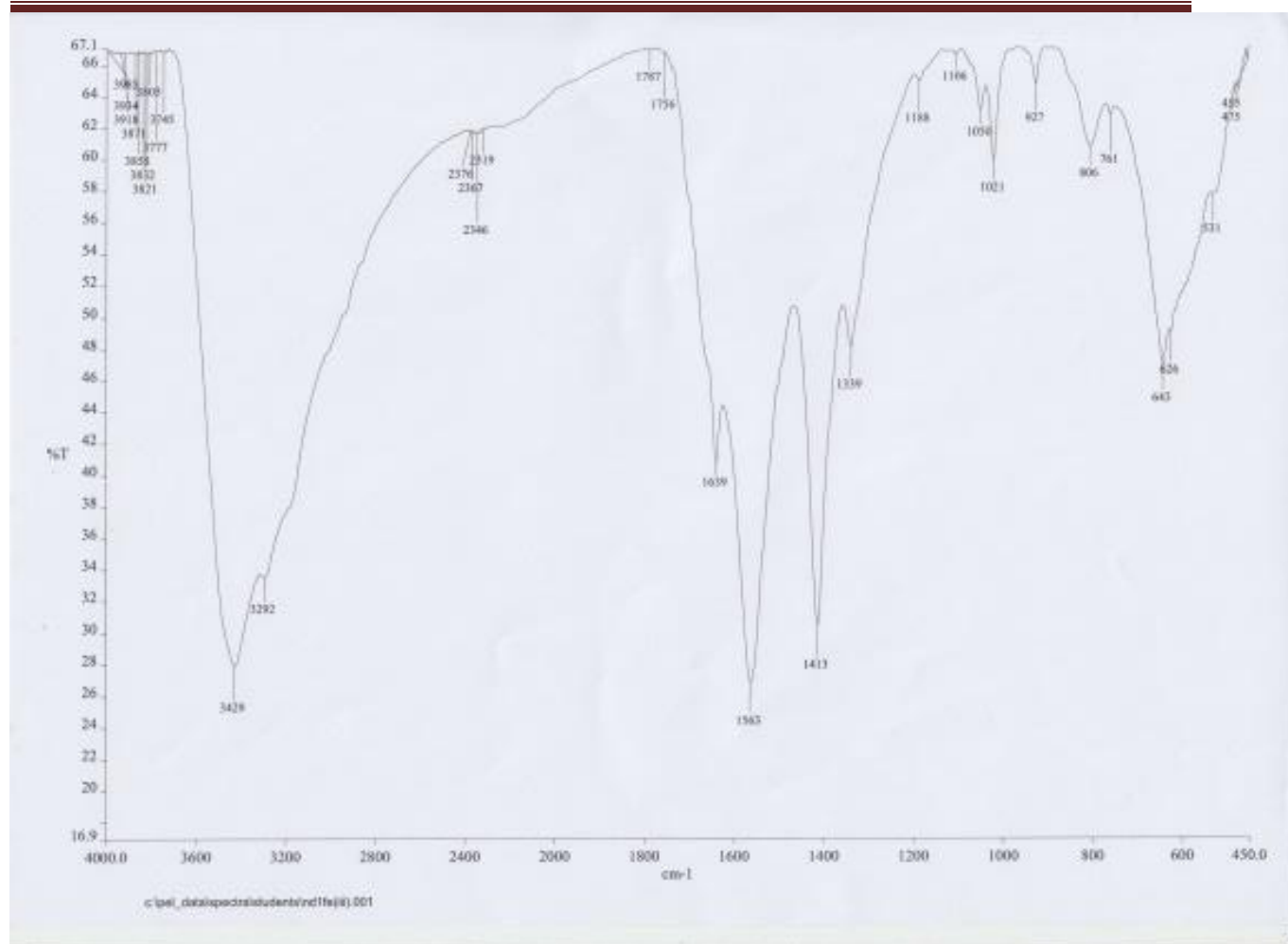


Fig. 6: IR Spectrum of [Fe(DPP)₂]Cl

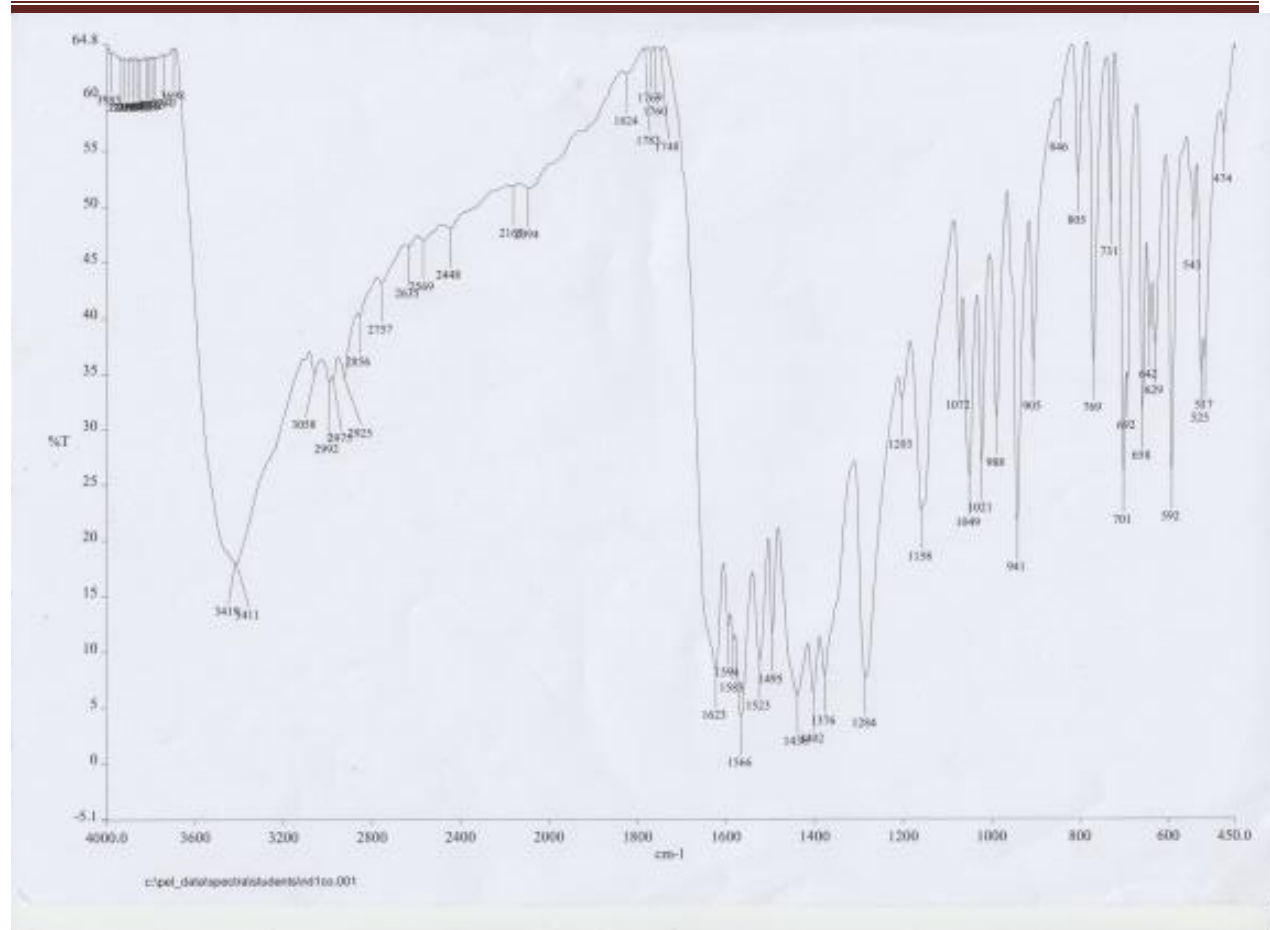


Fig. 7: IR Spectrum of [Co(DPP)₂]

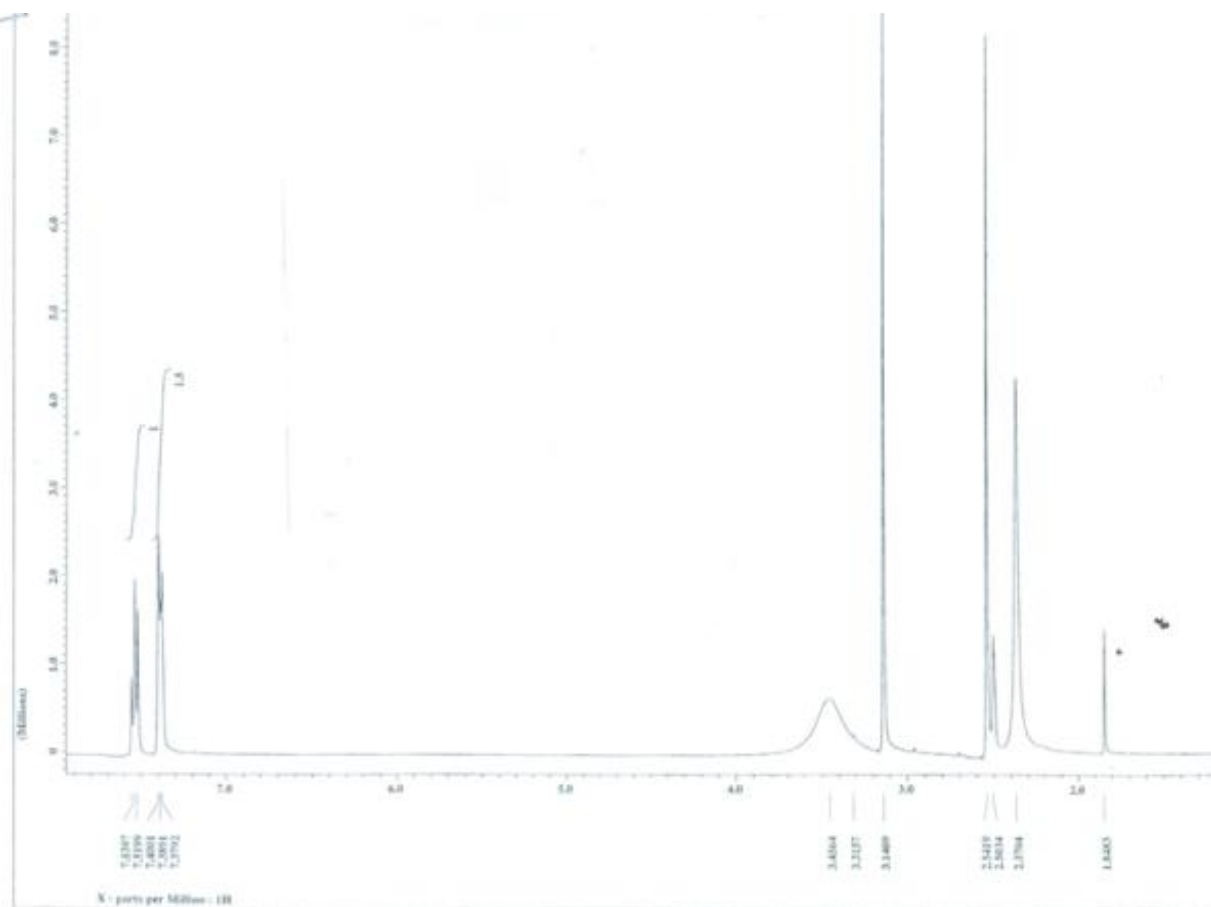


Fig 8: ¹H NMR Spectrum of HDPP

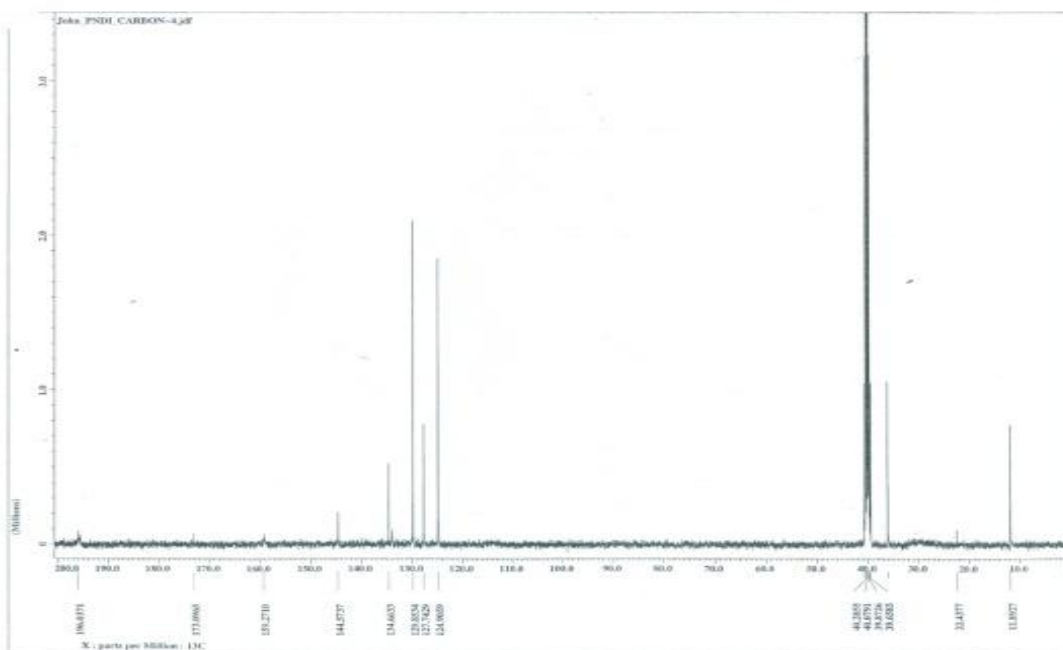


Fig 9: ¹³C NMR Spectrum of HDPP

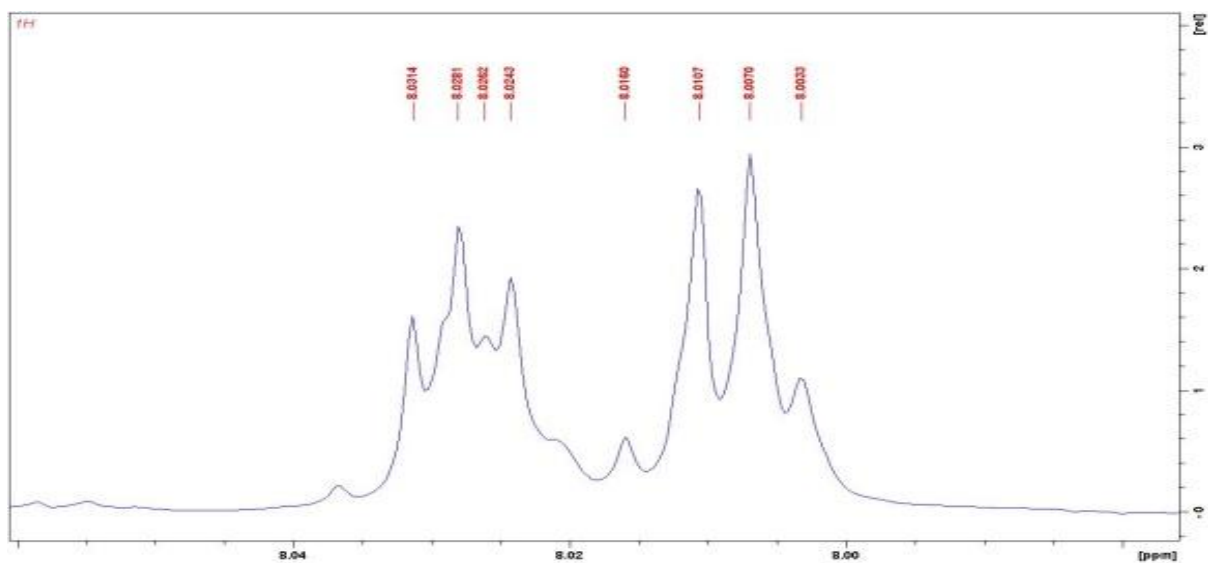


Fig 10: ¹H NMR Spectrum of [Fe(DPP)₂]Cl

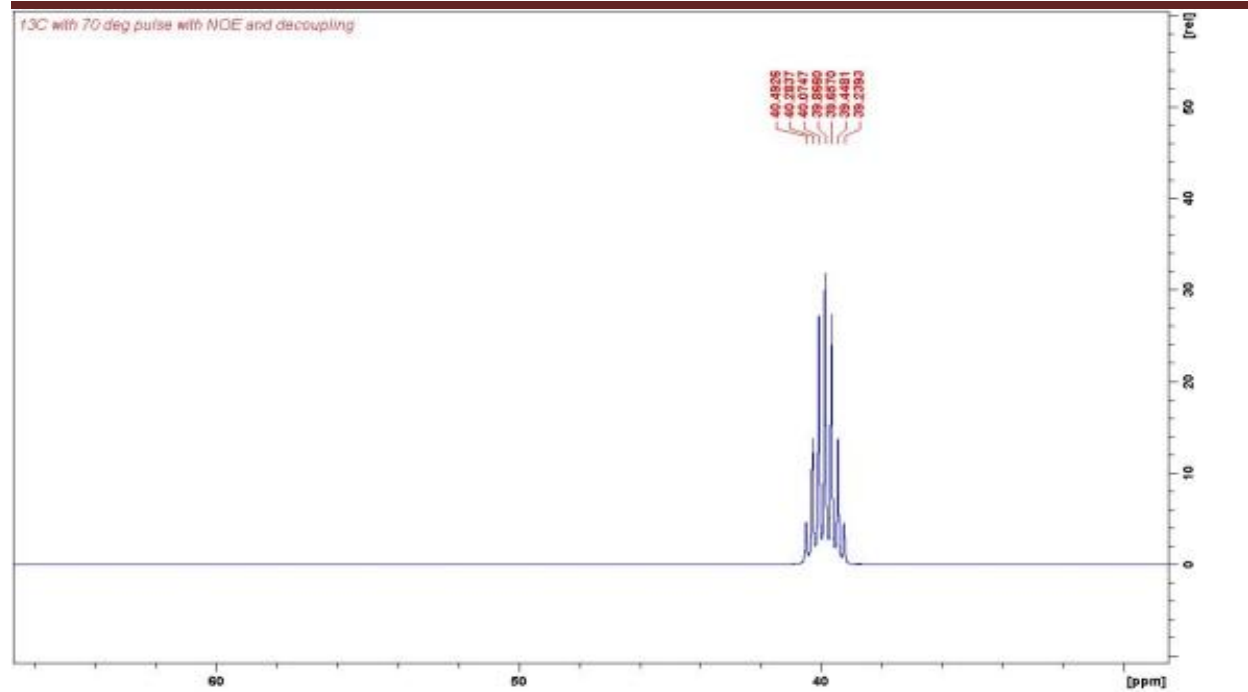


Fig 11: ¹³C- NMR Spectrum of Fe(DPP)₂Cl

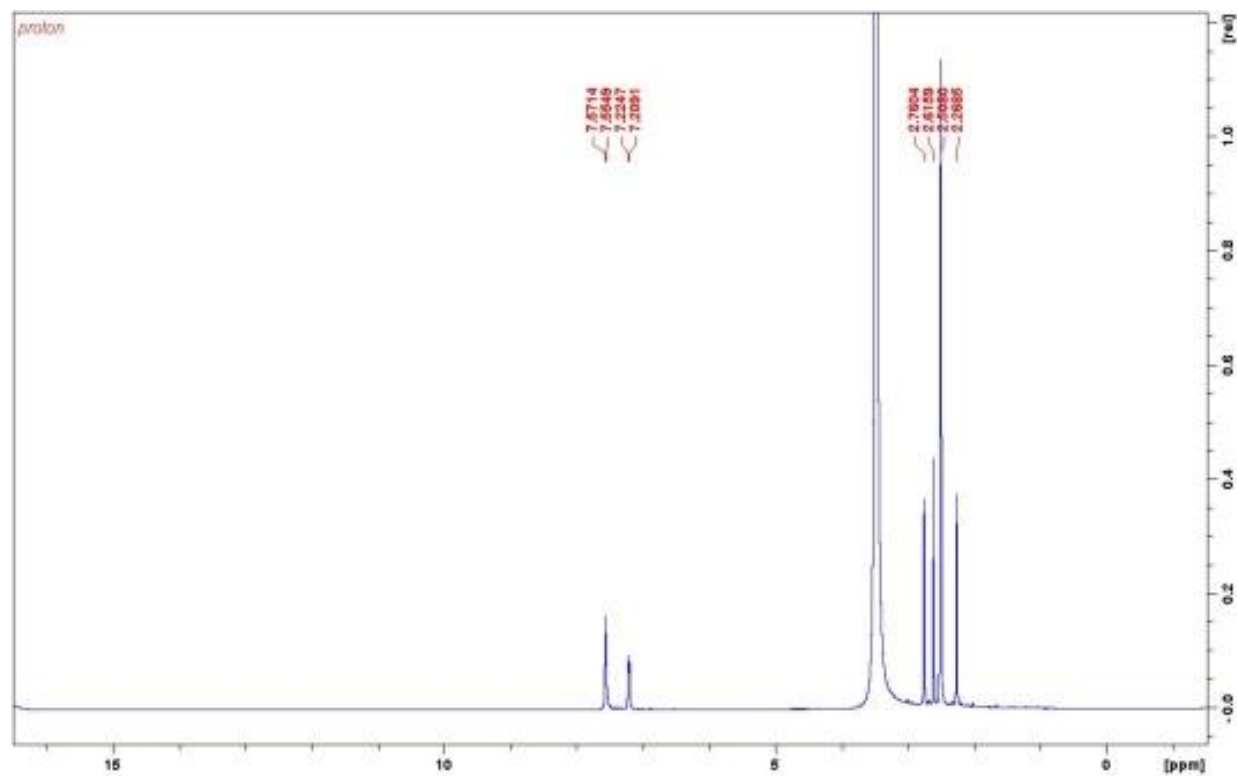


Fig 12: ¹H NMR Spectrum of [Co(DPP)]

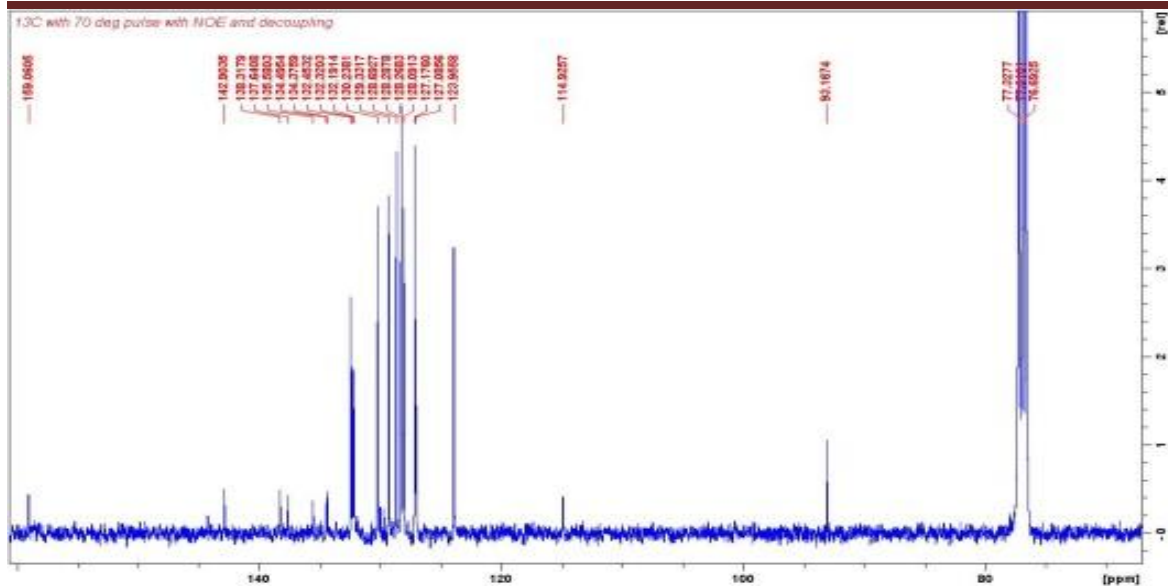


Fig 13: ¹³C NMR Spectrum of [Co(DPP)]